Prediction of flow stress of 7017 aluminium alloy under high strain rate compression at elevated temperatures

Ravindranadh BOBBILI*, B. RAMAKRISHNA, V. MADHU, A.K. GOGIA

Defence Metallurgical Research Laboratory, Hyderabad 500058, India

Abstract

An artificial neural network (ANN) constitutive model and Johnson—Cook (J—C) model were developed for 7017 aluminium alloy based on high strain rate data generated from split Hopkinson pressure bar (SHPB) experiments at various temperatures. A neural network configuration consists of both training and validation, which is effectively employed to predict flow stress. Temperature, strain rate and strain are considered as inputs, whereas flow stress is taken as output of the neural network. A comparative study on Johnson—Cook (J—C) model and neural network model was performed. It was observed that the developed neural network model could predict flow stress under various strain rates and temperatures. The experimental stress—strain data obtained from high strain rate compression tests using SHPB over a range of temperatures ($25°−300\ °C$), strains ($0.05−0.3$) and strain rates ($1500−4500\ s^{-1}$) were employed to formulate J—C model to predict the flow stress behaviour of 7017 aluminium alloy under high strain rate loading. The J—C model and the back-propagation ANN model were developed to predict the flow stress of 7017 aluminium alloy under high strain rates, and their predictability was evaluated in terms of correlation coefficient (R) and average absolute relative error (AARE). R and AARE for the J-C model are found to be 0.8461 and 10.624%, respectively, while R and AARE for the ANN model are 0.9995 and 2.58%, respectively. The predictions of ANN model are observed to be in consistent with the experimental data for all strain rates and temperatures.

1. Introduction

The mechanical properties as well as deformation and fracture mechanisms at high strain rates are quite different from those exhibited under quasi-static loading. Hence the accurate predictions may not be drawn from the quasi-static stress-strain data ($10^{-3}−10^{-1}\ s^{-1}$) at high strain rates ($10^2−10^7\ s^{-1}$), and the use of such data in the analysis and design of dynamically loaded structures may lead to erroneous conclusions and designs. It is therefore essential to study the material deformation characteristics at high strain rates for applications involving high strain rate deformations. The data obtained is helpful for the purpose of design of products as well as for developing the constitutive strength models of the materials. In order to develop more robust strength models and failure criteria under dynamic loading, more and more experimental data obtained over wide range of strain rates is required. An iterative procedure involving dynamic material testing and computer modelling may reduce the time and expense required for the development of advanced materials for applications such as armour. Characterization of deformation, fracture and load carrying capability of materials subjected to high strain rate is paramount for optimum material selection for design of armour materials which experience high strain rate dynamic deformation during impact of projectiles, blast loading, explosive forming and other impact events.

Various high strain rate test methods, such as drop weight, split Hopkinson pressure bar (SHPB), gas gun, Taylor impact and expanding ring, were reported in Refs. [1−5]. Split

* Corresponding author. Tel.: +40 24346332; fax: +40 24342252.
E-mail address: ravindranadhbobbili@gmail.com (R. BOBBILI).
Peer review under responsibility of China Ordnance Society.

Hopkinson pressure bar test method has been extensively used for testing in the strain rate regime of $10^2-10^4\ s^{-1}$ in tension and compression modes [2,3]. The three important considerations intrinsic to high strain rate testing are wave propagation, influence of strain rate on deformation of materials, and effect of high strain rate and temperature on properties of materials [2].

The effect of strain rate on material properties, viz., flow stress, strain rate sensitivity, etc., varies for each material. An increase in ductility of Al 7075 alloy was also reported by Magd et al. [2]. Metallographic investigations of the material showed ductile shear failure. Existence of two regions of strain rate sensitivity in Al 7075 over a range of strain rates was explained by Lee et al. [6]. It was reported that the strain rate has only slight effect on flow stress in the strain rate regime of $10^2-10^3\ s^{-1}$, which is higher than $10^3\ s^{-1}$ at strain rates, and the flow stress increases more rapidly with strain rate having an approximate linear relationship. Hou et al. [7] carried out the high strain rate experiments on Mg-Gd-Y alloy using SHPB over a range of temperatures. A modified J−C model was proposed to predict the dynamic response of this material over a wide range of strain rates and temperatures.

Ji et al. [8] carried out the hot compression tests on Aermet100 steel using Gleeble-3800 thermo-mechanical simulator to generate stress-strain data in a temperature range from 1073 to 1473 K and a strain rate range from 0.01 to 50 s^{-1}. The Arrhenius constitutive model and feed forward artificial neural network (ANN) model were developed to predict the high temperature deformation behaviour of the above material. ANN was found to be superior for modelling the high temperature deformation behaviours of materials. Han et al. [9] performed a comparative study on constitutive relationship of 904L Austenitic steel during hot deformation based on Arrhenius and ANN models. Experimental data were gathered from hot compression tests on Gleeble-1500D thermo-mechanical simulator to generate stress-strain data, in a temperature range from 1000 to 1150 °C and a strain rate from 0.01 to 10 s^{-1}. The back-propagation neural network model was proved to be more accurate and efficient in investigating the compressive deformation behaviour of material at higher temperatures. Sun et al. [10] employed ANN model to develop a constitutive model for the hot compression of Ti600 alloy. These tests were performed on Gleeble-1500 thermo-mechanical simulator in a temperature range from 800 to 1100 °C and a strain rate range from 0.001 to 10 s^{-1} to generate stress-strain data. ANN model provided a simple and efficient way to develop constitutive relationship for Ti600 alloy. Lin et al. [11] studied the compressive behaviour of 2124-T851 aluminium alloy under the strain rate from 0.01 to 10 s^{-1} and the temperature from 653 to 743 K using Gleeble-1500 thermo-mechanical simulation machine. A modified constitutive model accommodating the effects of material behaviour was proposed. Gupta [12] developed various semi-empirical models (Johnson−Cook model, modified Zerilli-Armstrong model and Arrhenius model) to study the effects of strain, strain rate and temperature. The tensiles of Austenitic stainless steel 316 were test using UTM machine at various strain rates (0.1−0.0001 s^{-1}) and temperatures (323−623 K). A

comparative study was undertaken among various constitutive models and ANN model.

The available literature has so far dealt with dynamic material characterization of various materials and their testing methodologies under different loading conditions, and microstructural analysis of various steels. So far no attempt has been made to study the effect of temperatures of 7017 aluminium alloy on dynamic properties using J−C and ANN models. The objective of the present study is to develop ANN model for predicting the dynamic flow stress of 7017 aluminium alloy under high strain rate loading conditions.

2. Experimental methods

2.1. Materials and test setup

The present alloy under study is Al-4.5 Zn-2.5 Mg-0.3Si-0.40 Fe (by weight %), commercially named as 7017 aluminium alloy. The quasi-static yield and ultimate tensile strengths of the alloy are 458 MPa and 508 MPa, respectively. Ductility measured as percentage elongation is 13% in 25 mm gage length. High strain rate compression testing of 7017 aluminium alloy samples with 3, 4, 5 mm in length and 6, 8, 10 mm in diameter was carried out using SHPB apparatus (Fig. 1). The specimens were prepared with L/D ratio of 0.5, so as to minimize the errors due to inertia and friction. Fig. 2 shows the dimensions and surface finish of compressed specimen used for 20 mm pressure bars. Length and diameter of the samples were changed to vary the strain rate.

The experimental stress−strain data were obtained from high strain rate compression tests using split Hopkinson pressure bar (SHPB), over a wide range of strains (0.05−0.3), strain rates (1500−4500 s^{-1}) and temperatures (25°−300 °C). The whole SHPB setup consists of pressure bars, gas gun which propels a striker bar for producing the compressive wave, strain gage for measuring the waves, associated mounting and alignment hardware, and associated instrumentation and data acquisition system. SHPB apparatus has two-pressure bars, one is called input or incident bar and another is called output or transmitted bar [7]. These pressure bars are made of materials having yield strength higher than that of the material to be tested. The specimen to be tested is sandwiched between the 2 bars. The yield strength of the pressure bar determines the maximum stress attainable within the deformed specimen, because the cross section of the specimen approaches to that of the pressure bar during
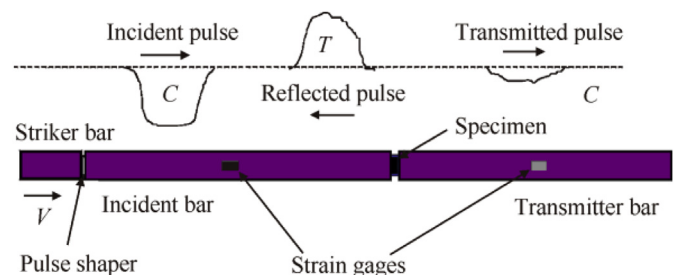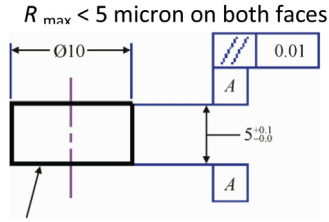

Fig. 1. Schematic diagram of Split Hopkinson pressure bar (SHPB).

R max < 5 micron on both faces

Ø10

0.01

A

$5^{+0.1}_{-0.0}$

A

Compression test sample for 20 mm bar

Fig. 2. Typical dimensions of high strain rate test samples.

deformation (Fig. 3). A rectangular compression wave with well-defined amplitude and length is generated in the incident bar when the striker bar strikes it.

The pressure wave was generated by having a striker bar (projectile) to impact the input (incident) pressure bar. The striker bar was propelled by a gas gun system attached at one end. The strain gages in conjunction with the amplifiers and associated instrumentation were used to record these wave pulses. Since the specimen deforms uniformly, the strain rate within the specimen is directly proportional to the amplitude of the reflected wave (ε_r).

Strain rate in the specimen is

$$\dot{\varepsilon} = \frac{-2c\varepsilon_r}{l} \tag{1}$$

Hence strain in the specimen is

$$\varepsilon = -\frac{2c}{l} \int_0^t \varepsilon_r dt \tag{2}$$

Stress in the specimen can be calculated as

$$\sigma = \frac{AE\varepsilon_t}{A_s} \tag{3}$$

where A and A_s are the areas of the bar and specimen, respectively; l is the length of specimen; c is wave speed; ε_t is the strain in the transmitted bar; and E is the elastic modulus of the pressure bar.

2.2. Johnson–Cook model

High strain rate plastic deformation of materials can be described by various constitutive equations that basically

Fig. 3. Schematic of the deformed specimen tested at a strain rate of 4500/s.

attempt to address the dependence of stress on strain, strain rate and temperature. In this regard, the stress can be presented as

$$\sigma = f(\varepsilon, \dot{\varepsilon}, T) \tag{4}$$

There are a number of equations that have been proposed to describe the plastic behaviour of materials as a function of strain rate and temperature. At low strain rates, the metals are known to work hardening along the well-known relationship, which is known as parabolic hardening and expressed as $\sigma = \sigma_o + k\,\varepsilon^n$, where σ_o is the yield stress, n is the work hardening exponent, and k is the pre-exponential factor.

The effect of strain rate on strength is generally expressed as: $\sigma \propto \ln\dot{\varepsilon}$. But the above relationship breaks down at strain rate above 10^2 s^{-1}.

The effects of temperature on the flow stress can be represented by

$$\sigma = \sigma_r \left[1 - \left(\frac{T - T_r}{T_m - T_r} \right)^m \right] \tag{5}$$

where T_m is the melting temperature; T_r is the reference temperature at which σ_r is the reference stress.

The dynamic flow stress depicting the effects of various parameters is expressed by Johnson–Cook model as

$$\sigma = \left(A + B\varepsilon^n \right) \left(1 + C \ln \dot{\varepsilon}^* \right) \left(1 - T^{*m} \right) \tag{6}$$

where A is the yield stress; B and n represent the effect of strain hardening; C is the strain rate constant; ε is the equivalent plastic strain; $\dot{\varepsilon}$ is the strain rate; $\dot{\varepsilon}^*$ is the dimensionless plastic strain rate represented as $\dot{\varepsilon}/\dot{\varepsilon}_o$ for $\dot{\varepsilon}_o = 1$ s^{-1}; T^* is the homologous temperature referred as $(T - T_{room})/(T_{melt} - T_{room})$; and m is the thermal softening factor. Thus, the terms presented in first, second and third brackets in Eq. (6) represent strain, strain rate and temperature effect, respectively. The J–C model is independent of pressure.

At reference strain rate and reference temperature, the functions of strain rate hardening and thermal softening are equal to unity, J–C model is simplified as follows

$$\sigma = A + B\varepsilon^n \tag{7}$$

where A is the yield stress which can be directly obtained from the strain-stress curve.

Plotting a line between $\ln \varepsilon$ and $\ln (\sigma - A)$ at the reference strain rate and reference temperature gives B and n in Eq. (7). Strain rate sensitivity C is determined as the slope of linear fit of log (strain rate) vs the dynamic flow stress/static stress using high strain rate data corresponding to a strain of 10%. The above constants are provided in the Table 1.

2.3. Artificial neural network approach

Neural networks are commonly employed in data prediction, categorization and data filtering applications. Artificial neural networks (ANN) imitate human brains to know the interaction between inputs and outputs through training.

Table 1
Johnson—Cook Model constants for Al 7017 alloy.

A/MPa	B/MPa	n	C	m
410	528	0.88	0.01024	0.6

Multi-layer ANN possesses input layers, hidden layers and output layers. The hidden layers located between input and output layers. The input layer first receives data and conveys it to the hidden layer for processing. The processed data is delivered as response to the output layer. Each layer can get a number of neurons connected by links with adaptable weights. These weights are adjusted during training. The inputs into a neuron are multiplied by their respective connection weights, and summed together, and a bias is added to the sum. This sum is converted through a transfer function to produce a single output. The nonlinear logarithmic sigmoid activation function was adopted in the hidden and output layers. The actual output obtained is compared to the required output to compute an error. The error for hidden layers is calculated by propagating back the error found out for the output layer; this technique is called back-propagation algorithm.

The experimental data were split into three sets, 70% for the training set, 15% for the verification set and 15% for the test set in ANN model. The input data (strain rate, strain and temperature) and output data (flow stress) were standardized in the range. The network model consists of ten hidden layers. To demonstrate the influence of network variables, the number of hidden layer neurons were varied from 10 to 40. It has been noticed that the predicted results are reasonable and accurate, with 15 neurons in each hidden layer.

3. Results and discussion

The experimental data obtained from the high strain rate compression tests (Fig. 4) on split Hopkinson pressure bar in a wide range of temperatures (25°—300 °C) and strain rates (1500—4500 s^{-1}) were employed to develop J—C model and ANN model for 7017 aluminium alloy. Fig. 5 depicts the comparison of the experimental results with the predicted

values at various strain rates and temperatures based on J—C strength model. It is observed that the predicted flow stress values obtained on J—C model are not consistent with the experimental values, particularly at high temperatures; the predicted values are smaller than the experimental results. So, J—C model is not so adequate in predicting the flow stress value in high temperature region. The predicting performance of the J—C model was evaluated by comparing the experimental and predicted data, as shown in Fig. 5. It was noticed that the J—C model could predict the experimental data only in the intermediate temperature range. This variation may be attributed to the error introduced by the fitting of the material constants at some conditions and the adiabatic temperature increment due to plastic deformation. Since J—C model is a phenomenological model, which does not consider the physical aspects of materials like theory of thermodynamics, thermally activated dislocation movement, and kinetics of slips while predicting the flow stress.

The J—C model and the back-propagation ANN model were developed to predict the flow stress of 7017 aluminium alloy under high strain rates and their predictability was evaluated in terms of correlation coefficient R and average absolute relative error (AARE). The predicted flow stresses of J—C model are given in Fig. 5. Fig 6 illustrates the flow stress predicted by ANN model versus measured value for testing set. R and AARE for the J-C model are found to be 0.8461 and 10.624%, respectively (Fig. 7), while R and AARE for the ANN model are 0.9995 and 2.58%, respectively (Fig. 8). It is found that the relative error obtained from the ANN model was observed to vary from 1.2% to 4.5%, while it was in the range of 4.2 %—10.6% for J—C model. The performance of the network also relies on learning parameters, such as the number of training epochs and the momentum, etc. To understand the significance of these parameters, the number of epochs is varied from 1000 to 10,000, the learning rate is varied from 0.1 to 0.9, and the momentum rate is varied from 0.1 to 0.8. It shows that the momentum rate does not exhibit a substantial influence on the performance of the network. It is established that the optimum number of epochs is about 12,000, the number of neurons in each hidden layer is 15, the
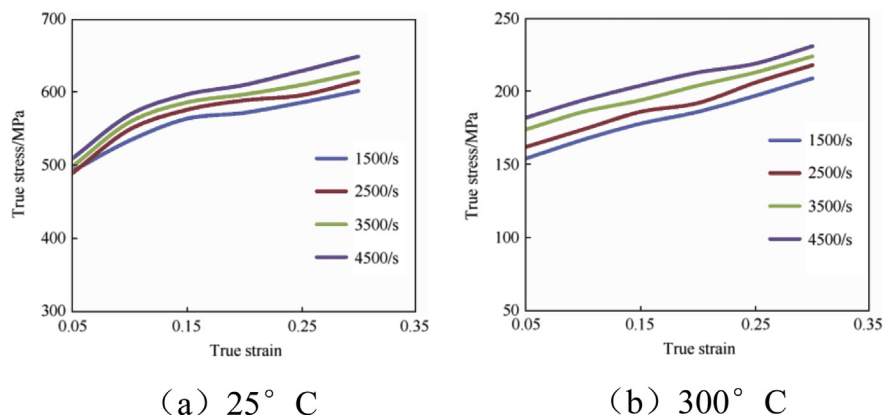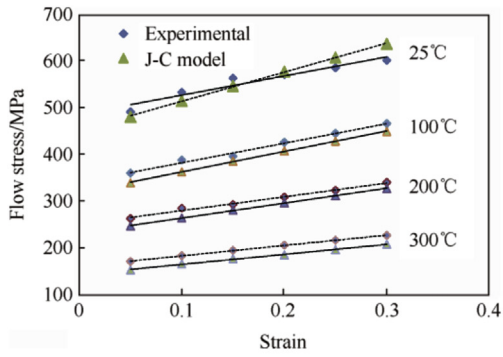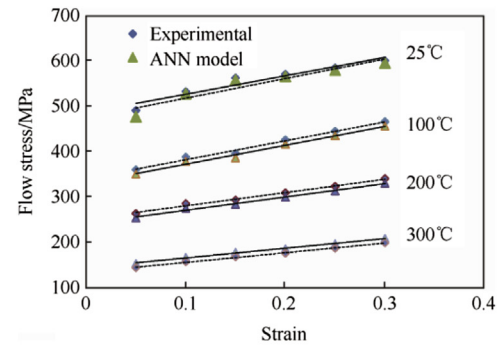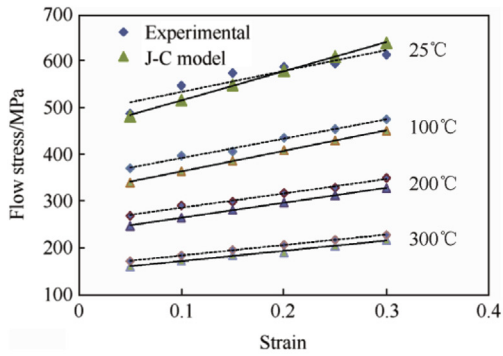

（a）25° C   （b）300° C

Fig. 4. True stress—strain curves of aluminium 7017 alloy at temperatures 25 °C and 300 °C.
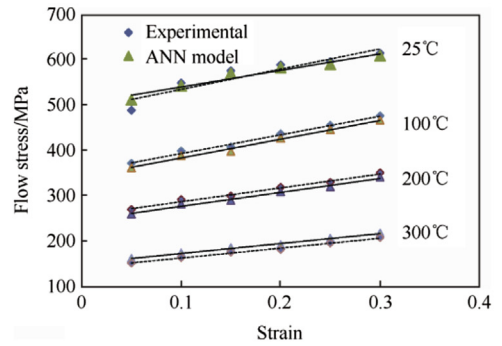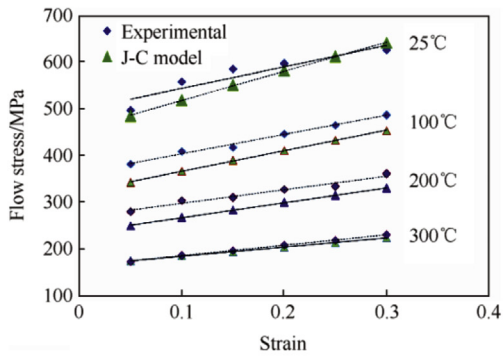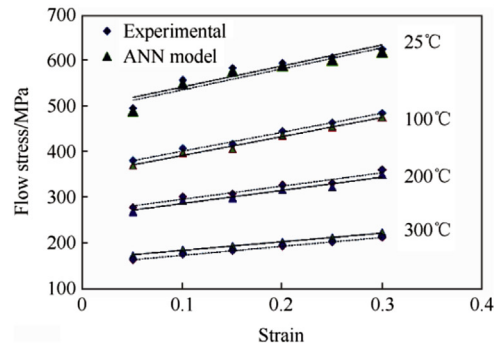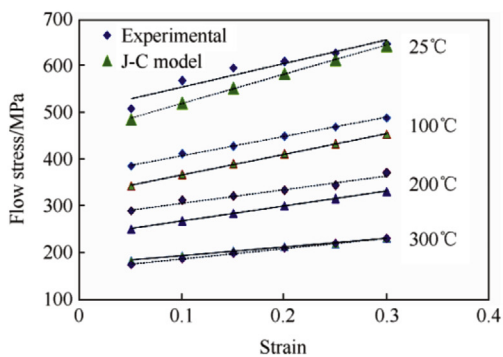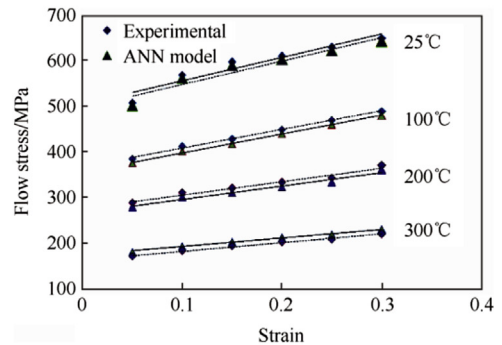
Fig. 5. Comparison between J–C Model and experimental flow stress of aluminium 7017 alloy by J–C model at strain rates.

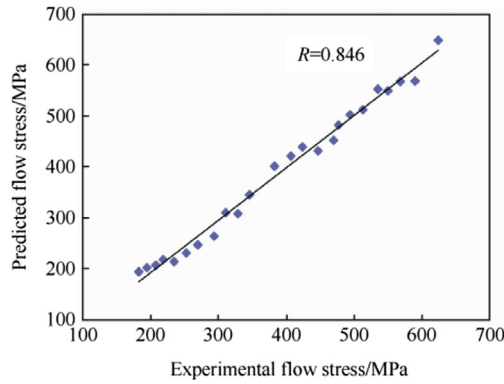Fig. 6. Comparison between ANN Model and experimental flow stress of aluminium 7017 alloy at strain rates.

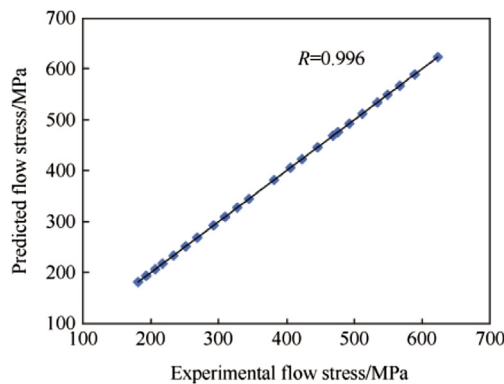Fig. 7. Plot of predicted vs. experimental for modified J−C model.

Fig. 8. Plot of predicted vs. experimental for ANN model.

number of hidden layers is 10, and the learning rate is 0.8, with a momentum of 0.7 in all layers. Mean square errors (MSEs) of desired and predicted data have been determined when MSE attained a minimum value of 0.001.

Hence, the data obtained in the ANN model were better compared to the J−C model. It shows that the developed ANN model can offer an efficient prediction of flow stress in the temperatures from 25 °C to 300 °C and strain rates from 1500 to 4500 s^{-1}.

4. Conclusions

This paper has made an attempt to study the comparison of the results obtained from J−C model and ANN model with experimental values. The following conclusions are drawn:

1) The J−C model and the back-propagation ANN model were developed to predict the flow stress of 7017 aluminium alloy under high strain rates, and their predictability was evaluated in terms of correlation coefficient R and average absolute relative error (AARE). R and AARE for the J−C model are found to be 0.8461 and 10.624%, respectively, while R and AARE for the ANN model are 0.9995 and 2.58%, respectively.

2) The established ANN model can effectively predict the experimental data over a wider range of temperatures and strain rates. This represents that ANN model has superior capability to model the dynamic behaviour of materials. This method circumvents the problems related to the constitutive models that involve the determination of more number of constants.

3) The validation tests have also been conducted to verify the results obtained by ANN technique. The predictions of the ANN model were in good agreement with the experimental data obtained from SHPB tests.

Acknowledgements

References

[1] Lee WS, Lin CF. Plastic deformation and fracture behaviour of Ti-6Al-4V alloy loaded with high strain rate under various temperatures. Mat Sci Eng A 1998;241(1−2):48−59.

[2] El-Magd E, Abouridouane A. Characterization, modeling and simulation of deformation and fracture behaviour of the light weight wrought alloys under high strain rate loading. Int J Impact Eng 2006;32:741−58.

[3] Mousavi ASH, Madaah-Hosseini HR, Bahrami. Flow stress optimization for 304 stainless steel under cold and warm compression by artificial neural network and genetic algorithm. J Mater Design 2007;28:609−15.

[4] Odeshi AG, Al-Ameeri S, Bassim MN. Effect of high strain rate on plastic deformation of a low alloy steel subjected to ballistic impact. J Mat Process Tech 2005;162-163:162−3.

[5] Mohr D, Gary G, Lundberg B. Evaluation of stress-strain curve estimates in dynamic experiments. Int J Impact Eng 2010;37:161−9.

[6] Lee WS, Sue WC, Lin CF, Wu CJ. The strain rate and temperature dependence of the dynamic impact properties of 7075 aluminium alloy. J Mat Process Tech 2000;100:116−22.

[7] Hou QY, Wang JT. A modified Johnson−Cook constitutive model for Mg-Gd-Y alloy extended to a wide range of temperatures. Comput Mater Sci 2010;50:147−52.

[8] Ji G, Li F, Li Q, Li H, Li Z. A comparative study on Arrhenius-type constitutive model and artificial neural network model to predict high-temperature deformation behavior in Aermet100 steel. J Mater Sci Engg A 2011;528:4774−82.

[9] Han Y, Qiao G, Sun J, Zou D. A comparative study on constitutive relationship of as-cast 904L austenitic stainless steel during hot deformation based on Arrhenius-type and artificial neural network models. Comput Mater Sci 2013;67:93−103.

[10] Sun Y, Zeng WD, Zhao YQ, Qi YL, Ma X, Han YF. Development of constitutive relationship model of Ti600 alloy using artificial neural network. Comput Mater Sci 2010;48:686−91.

[11] Lin YC, Xia YC, Chen XM, Chen MS. Constitutive descriptions for hot pressed 2124-T851 aluminium alloy over a wide range of temperature and strain rate. Comput Mater Sci 2010;50:227−33.

[12] Gupta AK, Anirudh VK, Singh SK. Development of constitutive models for dynamic strain aging regime in Austenitic stainless steel 304. Mater Des 2013;43:410−8.